The Astronomical Journal, 149:37 (8pp), 2015 February doi:10.1088/0004-6256/149/2/37

NEAR-INFRARED SPECTRA OF HIGH-ALBEDO OUTER MAIN-BELT ASTEROIDS*

Toshihiro Kasuga[1], Fumihiko Usui[2], Mai Shirahata[1,3], Daisuke Kuroda[4], Takafumi Ootsubo[5], Natsuko Okamura[6], and Sunao Hasegawa[3]
[1] National Institutes of Natural Science, National Astronomical Observatory of Japan, 2-21-1 Osawa, Mitaka, Tokyo, 181-8588, Japan; toshi.kasuga@nao.ac.jp
[2] Department of Astronomy, Graduate School of Science, The University of Tokyo, 7-3-1 Hongo, Bunkyo-ku, Tokyo 113-0033, Japan
[3] Institute of Space and Astronautical Science, Japan Aerospace Exploration Agency, 3-1-1 Yoshinodai, Sagamihara, Kanagawa 252-5210, Japan
[4] Okayama Astrophysical Observatory, National Astronomical Observatory of Japan, 3037-5 Honjo, Kamogata-cho, Asakuchi, Okayama 719-0232, Japan
[5] Department of Earth Science and Astronomy, Graduate School of Arts and Sciences, The University of Tokyo, 3-8-1 Komaba, Meguro-ku, Tokyo, 153-8902, Japan
[6] Department of Complexity Science & Engineering, The University of Tokyo Kiban Bldg. 408, 5-1-5 Kashiwanoha, Kashiwa, Chiba 277-8561, Japan
Received 2014 February 17; accepted 2014 September 2; published 2015 January 6

ABSTRACT

Most outer main-belt asteroids have low albedos because of their carbonaceouslike bodies. However, infrared satellite surveys have revealed that some asteroids have high albedos, which may suggest the presence of unusual surface minerals for those primitive objects. We present new near-infrared (1.1–2.5 μm) spectra of four outer main-belt asteroids with albedos $\geqslant 0.1$. The C-complex asteroids (555) Norma and (2542) Calpurnia are featureless and have (50%–60%) amorphous Mg pyroxenes that might explain the high albedos. Asteroids (701) Oriola (which is a C-complex asteroid) and (2670) Chuvashia (a D/T-type or M-type asteroid) show possible broad absorption bands (1.5–2.1 μm). The feature can be reproduced by either Mg-rich amorphous pyroxene (with 50%–60% and 80%–95% Mg, respectively) or orthopyroxene (crystalline silicate), which might be responsible for the high albedos. No absorption features of water ice (near 1.5 and 2.0 μm) are detected in the objects. We discuss the origin of high albedo components in the outer main-belt asteroids and their physical relations to comets.

Key words: infrared: planetary systems – minor planets, asteroids: general

Supporting material: data behind figures

1. INTRODUCTION

Primitive but unusually high albedo outer main-belt asteroids (those having a nearby semimajor axis $a \sim 3$ AU) have been reported by recent infrared studies with satellites (Tedesco et al. 2002; Ryan & Woodward 2010; Usui et al. 2013; Masiero et al. 2011, 2012, 2014). In this region, most objects are taxonomically classified as C or B types (Gradie & Tedesco 1982; DeMeo & Carry 2013). The reflective spectral slopes of these objects are nearly neutral and comparable with those of carbonaceous meteorites with low albedos (a few percent). Their aqueous alteration sequence is related to their spectral characteristics (e.g., Gaffey & McCord 1978; Bell et al. 1989; Gaffey et al. 1993; Hiroi et al. 1993, 1996), such as being incorporated as C-complex asteroids (C, B, F, and G types: Bus & Binzel 2002b). The presence of hydrated minerals and/or water ice in such objects is inferred. Absorption bands near 3 μm due to hydrated minerals or solid ice have been detected in the large asteroids (e.g., (1) Ceres, (24) Themis, and (65) Cybele; Jones et al. 1990; Vernazza et al. 2005; Campins et al. 2010; Rivkin & Emery 2010; Licandro et al. 2011; Takir & Emery 2012). Comet-like activity (sublimation of ice) is a potential reason for recurrent activities in a few kilometer-sized main-belt comets (Hsieh & Jewitt 2006; Jewitt 2012). For (1) Ceres, the photodissociation product of water (hydroxyl:OH) has actually been detected (A'Hearn & Feldman 1992; Küppers et al. 2014). On the other hand, non-primitive objects, such as V, S, and some X(M) types, comprise differentiated (high-temperature) and/or metamorphosed minerals that increase albedos (Kamei & Nakamura 2002; Weisberg et al. 2006; Fornasier et al. 2010). These objects primarily dominate the inner regions of the main belt (Gradie & Tedesco 1982; DeMeo & Carry 2013). Therefore, this raises the question of whether the high albedos of outer main-belt asteroids may offer unfamiliar, non-primitive materials that are not typically found in the outer main belt.

In a previous paper (Kasuga et al. 2013; hereafter, Paper I), we presented near-infrared (NIR) spectra of C complex outer main-belt asteroids with high albedos $p_v \geqslant 0.1$. Hapke models revealed that Mg-rich amorphous and/or crystalline silicates (high-temperature minerals) could be responsible for the high albedos (Paper I). The Mg-rich amorphous and/or crystalline silicate have also been detected in ice-rich comets (see the review by Wooden 2008). Spectral gradients of the nuclei are higher (redder) than those of C-complex objects, which taxonomically refer to D/T types (Tholen 1984; Bus 1999; Jewitt 2004; DeMeo & Binzel 2008). The spectra are generally featureless and hydrated reactions are rare (Jones et al. 1990), but some spectra infer an aqueous alteration and closely resemble those of the C-complex asteroids (known as gray Trojans; Bendjoya et al. 2004; Dotto et al. 2006; Szabó et al. 2007; Yang & Jewitt 2011; Yang et al. 2013). Their spectra are less red than those of usual cometary nuclei and Trojans (D/T types), but similar to those of dead comet candidates (Jewitt 2002, 2004; DeMeo & Binzel 2008; Lamy & Toth 2009; Kasuga et al. 2010). These traits imply that the nature of C-complex asteroids, D/T-type asteroids, and comets is comparable.

In this paper, we report new NIR observations of high albedo outer main-belt asteroids. Targets are from *AKARI*/AcuA[7] (Usui et al. 2011), in which the geometric albedos p_v, diameters D of objects, and the comparable taxonomic properties are

* Based on data collected at the Subaru Telescope, which is operated by the National Astronomical Observatory of Japan.

[7] http://darts.jaxa.jp/ir/akari/catalogue/AcuA.html

Table 1
Journal of Observations

Object	V^a	UT Date	r^b (AU)	Δ^c (AU)	α^d (deg)	Exp. Time (s)	Data[e]	Air Mass[f]	Standard	Air Mass[g]
(555) Norma	15.28	2013 Apr 6	3.051	2.082	5.7	180, 240	2 *JH*, 3 *HK*	1.15–1.17	(1)	1.07
(701) Oriola	14.77	2012 Nov 25	2.998	2.706	19.1	180	2 *JH*, 3 *HK*	1.03–1.07	(2)	1.02–1.04
(2542) Calpurnia	16.65	2013 Apr 6	2.953	2.371	17.7	180, 240	2 *JH*, 3 *HK*	1.00–1.02	(3)	1.07
(2670) Chuvashia	15.52	2013 Jan 5	2.938	2.082	11.2	180	2 *JH*, 2 *HK*	1.01–1.03	(4)	1.02

Notes. Standard stars (1) SA 107-684; (2) HD 79078; (3) SA 102-1081; (4) HIP 21852.
[a] Apparent visual magnitude, from NASA JPL Horizon.
[b] Heliocentric distance.
[c] Geocentric distance.
[d] Phase angle: Sun—Target—Observer.
[e] *ABBA* set.
[f] Air mass of asteroid.
[g] Air mass of standard star.

summarized. We study four asteroids: three C-complex asteroids and one that is either a D/T- or M-type asteroid. The principal question to address is whether their high albedo factors are the same as in those neutral, slightly reddish asteroids.

2. OBSERVATIONS

Observations were made using the 8.2 m diameter Subaru telescope at Maunakea, HI. We used the Infrared Camera and Spectrograph (IRCS; Tokunaga et al. 1998; Kobayashi et al. 2000) in its low-resolution grism spectroscopic mode. The IRCS comprises an Aladdin-III 1024 × 1024 InSb array at the Infrared Nasmyth focus (Terada et al. 2004). The image scale in the spectroscopic mode is 52 mas pixel^{-1}. The *JH* and *HK* prisms were used in their capable wavelength ranges of 1.1–1.6 μm and 1.4–2.5 μm, respectively. During the observations, the 188 element adaptive optics system was operated (Hayano et al. 2010; Minowa et al. 2010), giving a seeing range from 0.″2 to 0.″4 FWHM in the *K* band. We used slit widths of 0.″6 and 0.″9, which provided average spectral resolving powers of ~200 and ~130, respectively. A few sets of *ABBA* sequence were performed using two-position nodding patterns with an interval of 7″ along the slit. The two *AB* pairs of each sequence were combined to improve the signal-to-noise ratio (S/N). Non-sidereal tracking was used for asteroids. For use as telluric calibration standard stars, G types were taken close in time, transit, and air mass. The air mass difference between the asteroid and the standard star was selected to be as small as practical and less than 0.1. The observation log is given in Table 1.

The data were processed following the Subaru IRCS Data Reduction Cookbook.[8] The spectra of the asteroids and standard stars were corrected through flat fielding, bad pixel removal, and sky subtraction. Wavelength was calibrated using argon lines from an internal lamp. We applied an eight binned wavelength scale for one-dimensional spectra (see the cookbook). The reflective spectra were obtained by dividing the asteroids' spectra by the standard stars' spectra.

3. RESULTS AND ANALYSIS

Figure 1 shows the NIR spectra of the target asteroids (555) Norma, (701) Oriola, (2542) Calpurnia, and (2670) Chuvashia. We merged the *JH* and *HK* spectra, removed the excess wavelength coverage, and normalized these at 1.7 μm. Their visible spectra (<0.9 μm) (Tholen 1984; Bus & Binzel 2002b; Lazzaro et al. 2004) are not merged because of the absence of data from 0.9 to 1.1 μm. The data in shaded regions (1.35–1.45 μm, 1.8–1.95 μm) represent contamination by telluric absorptions. Small variations near 2.0 μm and uncertainties at longer wavelengths $\lambda > 2.3$ μm are residuals caused by imperfect telluric subtraction. Instrumental artifacts are found at ~1.1 and 1.25 μm. These are also reported in a previous study (Paper I).

The asteroids have nearly neutral to slightly red slopes from 1.1 to 2.5 μm. The objects are a few tens of kilometers in size with high albedos $p_v \geqslant 0.1$ (AcuA: Usui et al. 2011). The taxonomy is based on their visible spectra (Tholen 1984, 1989; Bus 1999; Bus & Binzel 2002a, 2002b; Hasselmann et al. 2012; summarized in the Appendix). They do not belong to any identified dynamical family (Novakovic 2011; Mothe-Diniz et al. 2012; Nesvorny 2012; Carruba 2013). The physical properties are summarized in Table 2. Asteroids (555) Norma and (2542) Calpurnia are featureless. On the other hand, the other two show broad absorption bands from 1.5 to 2.1 μm, as found in a previous work (Paper I). For asteroid (701) Oriola this feature is shallow, while for asteroid (2670) it is deep. They have three to four times higher albedos ($p_v \geqslant 0.2$) than the upper limit reported for primitive asteroids, p_v ($\approx p_R$) < 0.075 (Fernández et al. 2005). We find neither absorption bands of water ice at 1.5 and 2.0 μm nor those of hydrated minerals at 1.4 and 1.9 μm (Bishop & Pieters 1995). These depths of the characteristic bands can be reduced by material contamination or overlapped by atmospheric absorption bands, hiding their presence from spectroscopic detection (Clark & Lucey 1984). Absorption features near 0.7 μm through the aqueous alteration process (Vilas & Gaffey 1989; Rivkin et al. 2002; Bus & Binzel 2002b) are not clearly found in the data sets in the visible wavelength region (see the Appendix). Note that even if the 0.7 μm band cannot be seen, the 3 μm band can be detected when hydrated silicates are present (Rivkin et al. 2002). To limit results to the presence of hydrated silicates, the 3 μm absorption band is suggested for observation, but the sizes of objects are required to be on a 100 km scale for brightness (Rivkin et al. 2002).

As shown in Figure 2, we searched for our NIR spectral analogs using mixtures of various types of carbonaceous meteorites from de León et al. (2012; see also Paper I). The meteorite analogs are observationally determined for C-complex asteroids using the hydration rate, which is expressed as CI (Ivuna), CM (Mighei), Unusual CM, CV (Vigarano), CO (Ornans), or CK (Karoonda; de León et al. 2012). We find that

[8] http://subarutelescope.org/Observing/DataReduction/

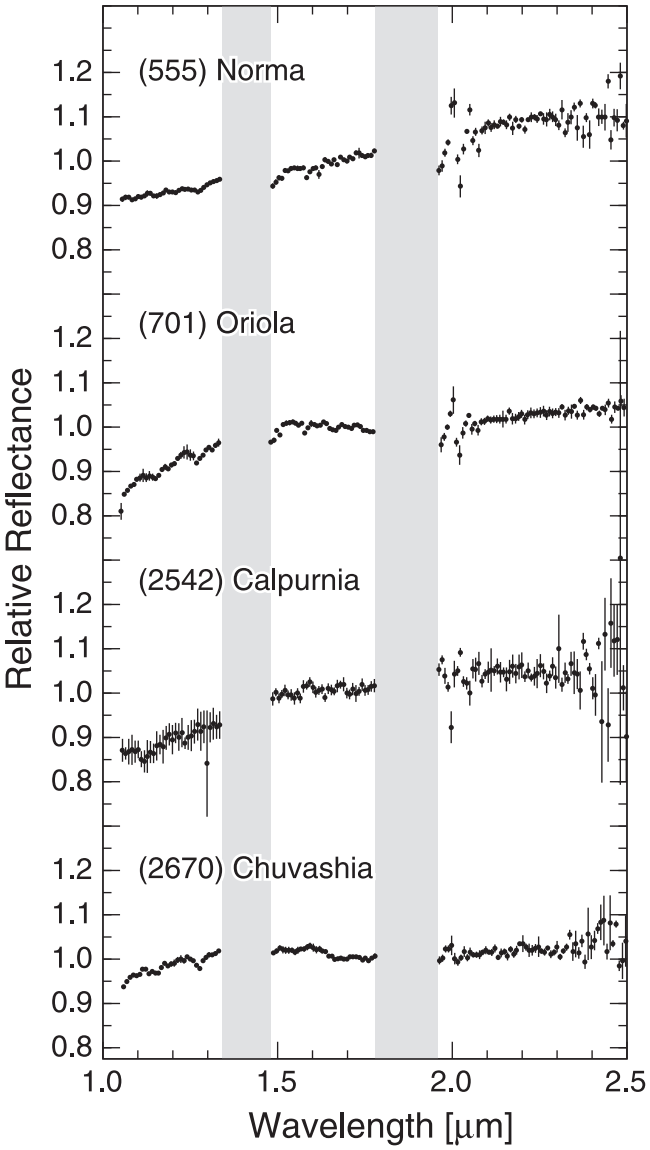

Figure 1. NIR spectra of the outer main-belt asteroids (555) Norma, (701) Oriola, (2542) Calpurnia, and (2670) Chuvashia. The data are normalized to 1.0 at 1.7 μm and vertically shifted.

NIR spectra of asteroids (555) Norma and (2670) Chuvashia are nearly in between the CI1/CM2 ~ Unusual CM meteorite groups. Spectral slopes of (701) Oriola and (2542) Calpurnia are redder than those of CI1/CM2, being rather D/T types (DeMeo et al. 2009). The NIR spectral gradients of gray D types are nearly neutral due to their aqueous environment, which is similar to those of C-complex asteroids (Yang & Jewitt 2011). Consequently, the targeted asteroids can be considered relatively hydrated carbonaceous bodies.

To identify the high-albedo component, we applied the Hapke model (Hapke 1981, 1993, 2012; Roush 1994) for reproducing the observed reflectance spectra. As noted in Paper I, we first tried with water-ice as one of components. The limit for the mass fraction was found to be only a few percent at most when none of the characteristic absorptions was detected, indicating that the contribution is negligibly small (from 1.1 to 2.5 μm). Therefore water-ice was not used in this study. Instead, we started with amorphous olivine (Aolv). The other two components were amorphous carbon (AC) and amorphous

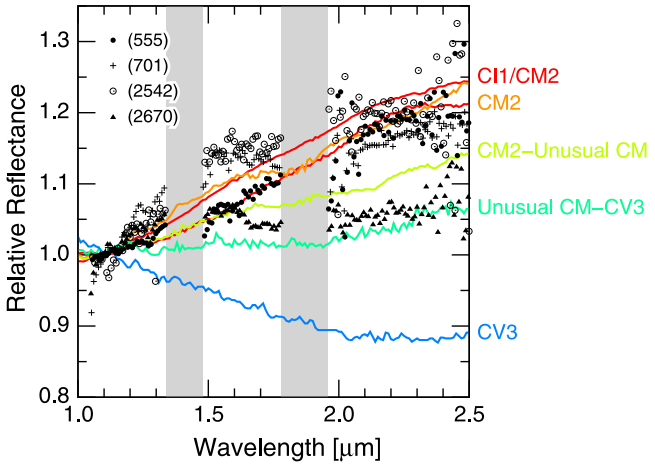

Figure 2. Comparison plots between the NIR spectra of the targeted asteroids and carbonaceous meteorite groups (de León et al. 2012), normalized at 1.1 μm to be unity (see Paper I). The spectra of (555) Norma and (2670) Chuvashia are approximately in the CI1/CM2 ~ Unusual CM groups, while those of (701) Oriola and (2542) Calpurnia are redder than any group. The latter two classifications are in slightly more hydrated phases of carbonaceous bodies.

pyroxene (Apyx) as they are reasonably common minerals in primitive asteroids (Cruikshank et al. 2001; Emery & Brown 2003, 2004; Yang & Jewitt 2007, 2010, 2011; Paper I). The optical constants of amorphous olivine ($MgFeSiO_4$) and amorphous pyroxene ($Mg_xFe_{(1-x)}SiO_3$, x = 0.4–0.95) were taken from Dorschner et al. (1995) and those of amorphous carbon were from Rouleau & Martin (1991). The reflective spectral model is controlled by the weight fractions of the total amount of neutral material, the Mg/Fe ratio in pyroxene, and the grain size of each component (Hanner 1999; Yang & Jewitt 2007). In the model, the grain size is assumed to be the same for all components. We varied Mg content in pyroxene in the ranges of 40%, 50%, 60%, 70%, 80%, and 95% Mg and derived a goodness of fit for each case using the reduced χ-squared value: $\chi_\nu^2 = \sum_i^n [(y^i_{\rm obs} - y^i_{\rm model})/y^i_{\rm err}]^2$, where $y^i_{\rm obs}$ is the observed reflectance spectra, $y^i_{\rm model}$ is the computed reflectance spectra, $y^i_{\rm err}$ is the uncertainty in $y^i_{\rm obs}$, and the summation is carried out over the i data points (see Paper I). The fuzzy wavelength regions (1.1 μm, 1.25 μm, 1.35–1.45 μm, 1.8–1.95 μm and 2.3 μm $< \lambda$, as noted earlier) were not used for the fitting. The results of the spectral models are shown in Tables 3 and Figures 3, 4(a), 5 and 6(a).

The models successfully fit the spectral profiles of the featureless asteroids (555) Norma and (2542) Calpurnia. For example, (555) Norma is well fitted by the model with Aolv 40 % by weight, 50%–60% Mg content in Apyx, and grain size $D \sim 5$ μm ($\chi_\nu^2 \lesssim 4.3$ in Table 3), presented in Figure 3. On the other hand, we can improve the model for the featured asteroids (701) Oriola and (2670) Chuvashia for their possible weak absorption bands. Those bands are similar to a feature of crystalline silicate (orthopyroxene; noted in Paper I). Then we attempted orthopyroxene (Opyx: $Mg_{0.7}Fe_{0.3}SiO_3$) with optical constants from laboratory experiments (Pollack et al. 1994) shown as a green curve in Figures 4(b) and 6(b). The Opyx model reproduced the absorption bands of the featured asteroids with a smaller χ_ν^2 than the Apyx model (see Table 4).

Table 2
Physical Properties

Object	a[a] (AU)	e[b]	i[c] (deg)	D[d] (km)	p_v[e]	Type[f]
(555) Norma	3.188	0.150	2.646	32 ± 1	0.10 ± 0.01	B[(1)]
(701) Oriola	3.013	0.032	7.142	39 ± 1	0.24 ± 0.02	C[(2)]
(2542) Calpurnia	3.130	0.073	4.621	18 ± 1	0.15 ± 0.02	C[(3)]
(2670) Chuvashia	3.173	0.076	9.856	20 ± 1	0.30 ± 0.02	D/T, M[(4)]

Notes. Orbital data from JPL/Horizon. Diameters and geometric albedos from *AKARI*/AcuA (Usui et al. 2011).
[a] Semimajor axis.
[b] Eccentricity.
[c] Inclination.
[d] Diameter.
[e] Geometric albedo in optical.
[f] Taxonomy ($\lambda < 1.1$ μm) from (1) Bus (1999), Bus & Binzel (2002a), Bus & Binzel (2002b), (2) Bowell et al. (1979), Tholen (1984, 1989), (3) Hasselmann et al. (2012) and (4) this work, summarized in the Appendix.

Table 3
Model Fits I

Object	Aolv[a] (wt.%)	AC[b] (wt.%)	Apyx[c] (wt.%)	Mg in Apyx (%)	Grain Size (μm)	χ_ν^{2}[d]
(555) Norma	43	39	18	40	5	4.634
	42	40	18	50	4	4.037
	43	32	25	60	5	4.251
	34	20	46	70	3	4.356
	27	10	63	80	5	4.486
	8	0	92	95	2	5.984
(701) Oriola	0	43	57	40	2	6.640
	0	39	61	50	3	4.981
	0	28	72	60	3	4.388
	0	7	93	70	3	5.993
	0	7	93	80	6	6.073
	1	0	99	95	40	11.842
(2542) Calpurnia	0	54	46	40	3	2.465
	0	43	57	50	3	2.386
	0	31	69	60	4	2.314
	0	19	81	70	5	2.533
	0	11	89	80	6	2.525
	0	5	95	95	16	2.446
(2670) Chuvashia	0	93	7	40	5	3.298
	0	91	9	50	5	3.143
	95	0	5	60	40	3.112
	94	0	6	70	40	3.090
	93	0	7	80	40	3.016
	83	0	17	95	40	3.063

Notes. Parameters are given by weight fractions of amorphous olivin, amorphous carbon, and amorphous pyroxene with different Mg content (40%, 50%, 60%, 70%, 80%, and 95% Mg).
[a] Amorphous olivin (50% Mg).
[b] Amorphous carbon.
[c] Amorphous pyroxene.
[d] Reduced χ-squared value.

4. DISCUSSION

Our models find a relatively Mg-rich amorphous pyroxene composition. We also find possible orthopyroxene absorption features in asteroids (701) Oriola and (2670) Chuvashia with $p_v \geqslant 0.2$. The high albedos of these asteroids may be explained by their high Mg silicates (Emery & Brown 2004; Lucey & Noble 2008). Also, the albedos of high-temperature minerals (e.g., crystalline silicates) in differentiated objects and the inclusion of such material in meteorite samples are known to be high (Kamei & Nakamura 2002; Weisberg et al. 2006). Even if (2670) was an M-type asteroid, it should also be considered whether it has differentiated or primitive aspects among the large variety of spectral properties (Fornasier et al. 2010). Therefore, we again report that moderate Mg-rich amorphous or crystalline silicates can be

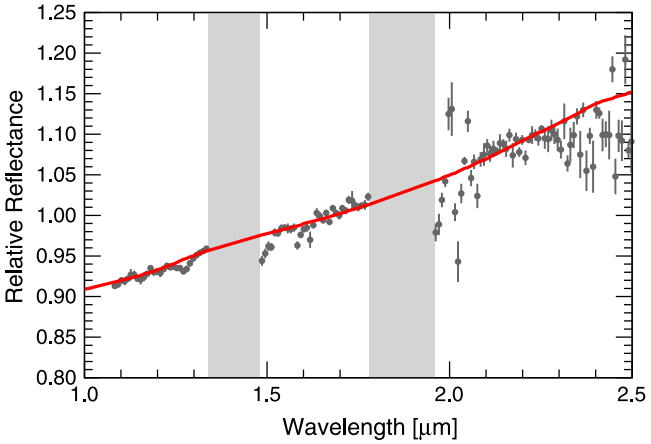

Figure 3. NIR spectrum of (555) Norma (black) and the best-fit model spectrum (red) using weight fractions of 42% Aolv, 40% AC, 18% Apyx (with 50% Mg), and a grain size of 4 μm ($\chi_\nu^2 \sim 4.037$). The spectra are reduced be relative reflectance scaled to 1.0 at 1.7 μm. The data used to create this figure are available.

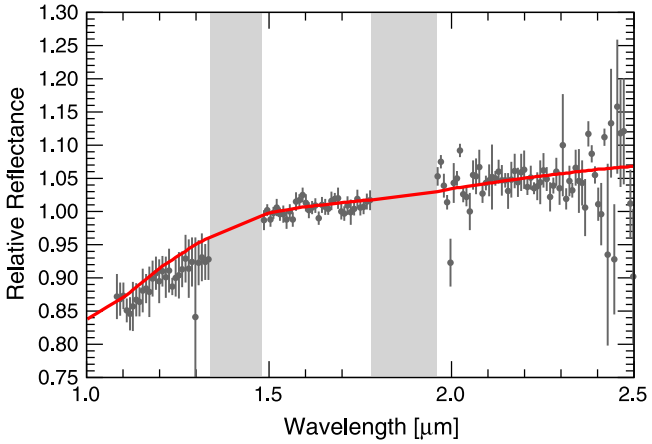

Figure 5. Same as Figure 3 but for asteroid (2542) Calpurnia. The observed feature is reproduced in red (weight fractions of 0% Aolv, 31% AC, and 69% Apyx (60% Mg content) with grain size of 4 μm, $\chi_\nu^2 \sim 2.314$). The data used to create this figure are available.

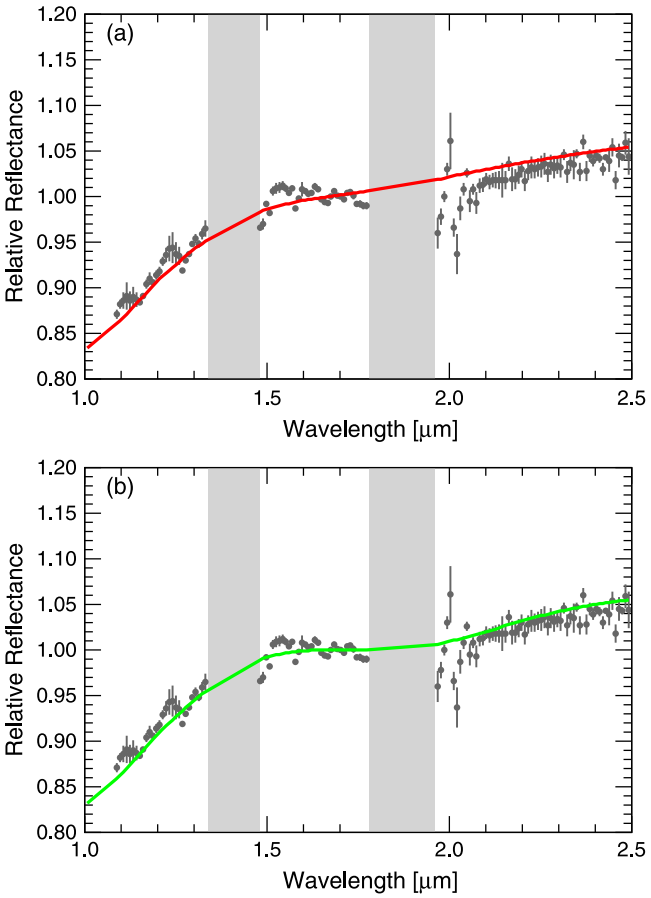

Figure 4. Top panel (a): the same as Figure 3 but for asteroid (701) Oriola, which is fitted by the model (red) 0% Aolv, 28% AC, 72% Apyx (with 60% Mg) by weight and a grain size of 3 μm ($\chi_\nu^2 \sim 4.388$). The bottom panel (b) is fitted by the model (green) 35% Opyx, 12% AC and 53% Apyx (with 60% Mg) by weight and a grain size of 2 μm ($\chi_\nu^2 \sim 3.554$). The data used to create this figure are available.

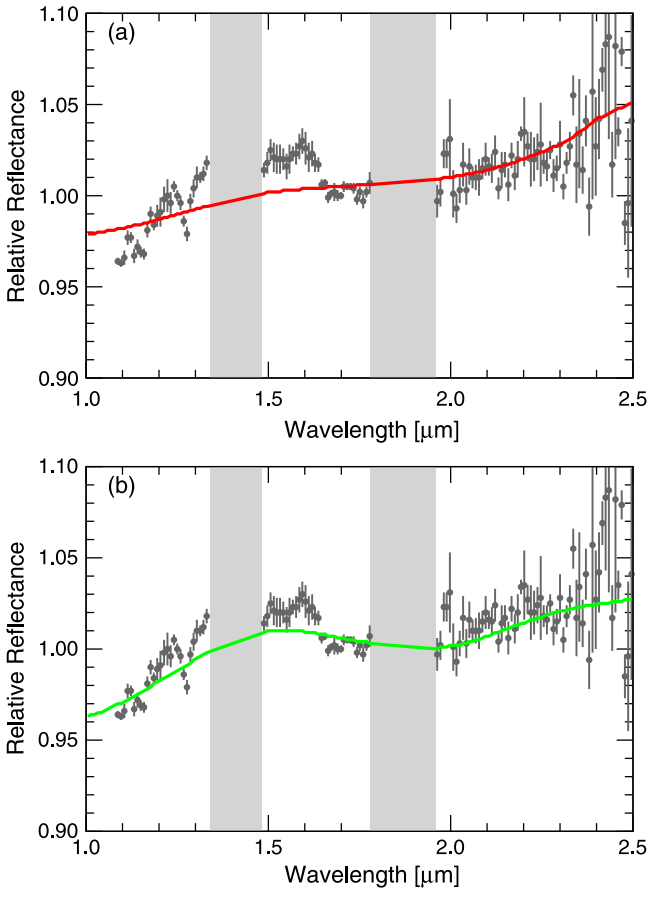

Figure 6. Upper panel (a): NIR spectrum of (2670) Chuvashia (black) and the model (red) using 93% Aolv, 0% AC, and 7% Apyx (with 80% Mg) by weight and a grain size of 40 μm ($\chi_\nu^2 \sim 3.016$). The lower panel (b) is fitted by the model (green) 45% Opyx, 55% AC, and 0% Apyx by weight and a grain size of 4 μm ($\chi_\nu^2 \sim 2.233$). These data are normalized to 1.0 at 1.7 μm. The data used to create this figure are available.

factors causing high albedos. The results are consistent with those in our previous study (Paper I).

Asteroids and comets are similar in their Mg-rich content and high-temperature minerals. The presence of Mg-rich minerals has been confirmed in comets (Wooden 2008). Meteoroids in meteor streams whose origins are asteroids and (short-period) comets provide Mg-rich abundances in metals (e.g., Geminids, Leonids; Kasuga et al. 2005a, 2005b). High-temperature minerals (e.g.,

Table 4
Model Fits II

Object	Opyx[a] (wt.%)	AC[b] (wt.%)	Apyx[c] (wt.%)	Mg in Apyx (%)	Grain Size (μm)	χ_ν^{2d}
(701) Oriola	35	12	53	60	2	3.554
(2670) Chuvashia	45	55	0	⋯	4	2.233

Notes. Parameters are given by weight fractions of water-ice, amorphous carbon, and amorphous pyroxene with different Mg content (40%, 50%, 60%, 70%, 80%, and 95% Mg).
[a] Ortho pyxroxene (70% Mg).
[b] Amorphous carbon.
[c] Amorphous pyroxene.
[d] Reduced χ-squared value.

crystalline silicates, chondrules, calcium–aluminum-rich inclusions) are typically found in comets (Brownlee et al. 2006; Wooden 2008). The best-fit models herein show crystalline silicates in some asteroids, as generally found in comets (Wooden 2008). The oxygen isotope compositions in chondrule-like materials returned from comet 81P/Wild-2 show similarities to those of chondrules in carbonaceous meteorites (Nakamura et al. 2008). This study may increase the evidence of their similarities (see also Paper I).

Aqueous alteration could be conceivable on both asteroids and comets. For asteroids with sizes of 10 km $< D <$ 1000 km, short-lived radionuclides (e.g., ^{26}Al) are the primary heat sources for ice melting ($T <$ 570 K: McSween et al. 2002; Brearley 2006, and references therein). The large bodies can contain liquid water that is in close contact to anhydrous silicates processing into hydrated silicates (McSween et al. 2002; Brearley 2006). They are presumed to be in C-complex (see the reviews by Rivkin et al. 2002; Jewitt et al. 2007) and gray D/T-type asteroids (Bendjoya et al. 2004; Dotto et al. 2006; Szabó et al. 2007; Yang & Jewitt 2010, 2011; Yang et al. 2013). For ice-rich comets (D/T types), on the other hand, the mechanism is unattainable. The size of most nuclei is on the kilometer-scale (Lamy et al. 2004), which is too small for ice to melt in the nuclei by radiogenic heating (Prialnik & Podolak 1999; Merk & Prialnik 2006; Prialnik et al. 2008; McKinnon et al. 2008; Kelley & Wooden 2009). The presence of highly volatile molecules such as CO and CO_2 suggests that comet interiors have remained frozen, at low temperatures <30 K–70 K, since their formation (Yamamoto 1985; Ootsubo et al. 2012). For this reason, a fluid condition (e.g., liquid water) is particularly rare in comets (Jessberger 1999; Brownlee et al. 2006; Zolensky et al. 2006, 2008; Kelley & Wooden 2009). Nevertheless, some possible evidence for aqueous products has been reported. Phyllosilicates and carbonates were detected in the ejecta of comet 9P/Tempel 1 by Deep Impact (Lisse et al. 2006). Other secondary minerals (hydrated sulfides) were found in the Stardust samples from comet 81P/Wild 2 (Berger et al. 2011). By laboratory experiment, Nakamura-Messenger et al. (2011) revealed that cometary anhydrous interplanetary dust particles are highly susceptible to aqueous alteration, even at low temperatures (270 K–300 K), for a short time (hours to weeks). Since some fluid conditions could be present in the near-surface cometary mantles (e.g., interfacial water layers; Rietmeijer 1985; Berger et al. 2011; Miles & Faillace 2012), aqueous alteration would be allowed (Nakamura-Messenger et al. 2011). Following from this, asteroids with less red spectra are presumed to be hydrated comet-like bodies. Namely, they partly share the features of comets. This may imply a physical evolution relation between asteroids and comets.

Impacts can alter the surface properties of asteroids. Localized albedo changes near craters (from 0.5 to 2 times compared to the background) are found in (4) Vesta, which could be mixed with dark and/or melted material of projectiles (Hasegawa et al. 2003; McCord et al. 2012). Recently, the large scale outer main-belt asteroid (596) Scheila ($a \sim 2.9$ AU), which has a T-type spectrum (DeMeo et al. 2009), was impacted by a small asteroid with $D \sim 40$ m (Jewitt et al. 2011; Ishiguro et al. 2011) (cf. $D \leqslant 100$ m; Bodewits et al. 2011). The event apparently altered the optical properties of the surface (given by the light curve) and increased the albedo by a factor of ∼2 (Bodewits et al. 2014). The affected area is 10 times larger compared to the crater size of $D \sim 100$ m (Bodewits et al. 2014). Therefore, sub-catastrophic collisions can be taken into account in a primitive-surface renewal process. Here, we examine the possibility for our target asteroids. The impact timescale between asteroids in the main belt, τ_c, can be derived from $\tau_c = 2600\ (D_p/1\ \mathrm{m})^{2.7}\ (D_t/1\ \mathrm{km})^{-2}$ (year) using D_p, the diameter of projectiles, and D_t, the diameter of the target asteroids (Jewitt 2012). With $D_p \sim 40$ m (see the Scheila case) and $D_t =$ 10–50 km, we find $\tau_c \sim 10^{4-5}$ year. This is much shorter than the solar system age of 10^9 year. The number of asteroids integrated over the size distribution in the main belt is given by Jewitt (2012), $N_t\ (\geqslant D_t) = 1.69 \times 10^{14}\ (D_t/1\ \mathrm{m})^{-2.7}$. By substituting this into $D_t =$ 10–50 km and with $\tau_c \sim 10^{4-5}$ year, we find that, in the main belt, similar events occur every 200–500 years. Thus, impacts are not ruled out as causing the high albedos of primitive asteroids.

Lastly, the 3 μm IR data are critical for measuring and constraining the presence and distribution of volatiles. For 100 km sized outer main-belt asteroids with low albedos, categorization of the 3 μm absorption bands is being attempted using their depths and shapes (Rivkin et al. 2012a, 2012b). In the future, advanced telescope technology will enable us to investigate them even for 10 km sized asteroids. Such studies help us to understand the nature of potentially water-related asteroids.

5. SUMMARY

We report NIR spectroscopic observations of four high albedo outer main-belt asteroids, (555) Norma, (701) Oriola, (2542) Calpurnia, and (2670) Chuvashia. We find that

1. The featureless asteroids (555) Norma and (2542) Calpurnia are best fitted with a spectral model using amorphous pyroxene with 50%–60% Mg. The results imply that moderately Mg-rich silicates are responsible for the high albedos of these C-complex asteroids.
2. The high albedos in (701) Oriola (a C-complex asteroid) and (2670) Chuvashia (a D/T-type or M-type asteroid) can be explained by Mg-rich amorphous pyroxene with 50%–60% and 80%–95% Mg, respectively. Orthopyroxene (crystalline silicate) could also be present.

Toshi Kasuga acknowledges Prof. Kathrin Altwegg for her encouragement of this work at the University of Bern. We thank Hideyo Kawakita, Tomoko Arai, Keiko Nakamura-Messenger, and David Jewitt for discussions. T. K. is financially supported by the NAOJ Overseas Visit Program

for Young Researchers. D. K. is supported by the Optical & Near-Infrared Astronomy Inter-University Cooperation Program, the MEXT of Japan. T. O. is supported in part by JSPS KAKENHI Grant Number 25400220. S. H. is supported by the Space Plasma Laboratory, ISAS/JAXA. Taxonomic type results presented in this work were determined, in whole or in part, using the Bus–DeMeo Taxonomy Classification Web tool by Stephen M. Slivan, developed at MIT with the support of National Science Foundation Grant 0506716 and NASA Grant NAG5-12355. The data herein were obtained at the NAOJ Subaru Telescope with assistance from Miki Ishii and Michael Lemmen. We appreciate the informative comments from the anonymous reviewer.

APPENDIX

We present a set of information in the visible spectral region of observed asteroids. Figures A1 , A2 , and A3 show (555) Norma with SMASS II (Bus 1999; Bus & Binzel 2002a, 2002b), (701) Oriola with *UBV* colors (Bowell et al. 1979; Tholen 1984), and (2542) Calpurnia with SDSS (Hasselmann et al. 2012), respectively.

For the taxonomy of asteroid (2670) Chuvashia, a supplemental observation was taken on the night of UT 2014 January

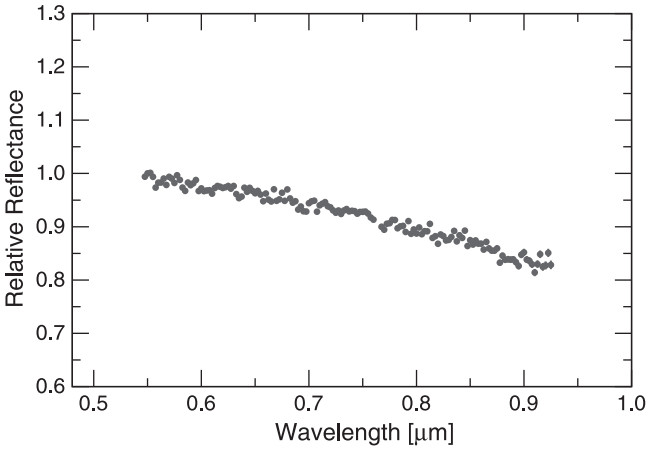

Figure A1. Visual spectrum of asteroid (555) Norma, taken by SMASS II (Bus 1999; Bus & Binzel 2002a, 2002b). The data are normalized to be 1.0 at 0.55 μm. The negative slope corresponds to that of a B-type asteroid.

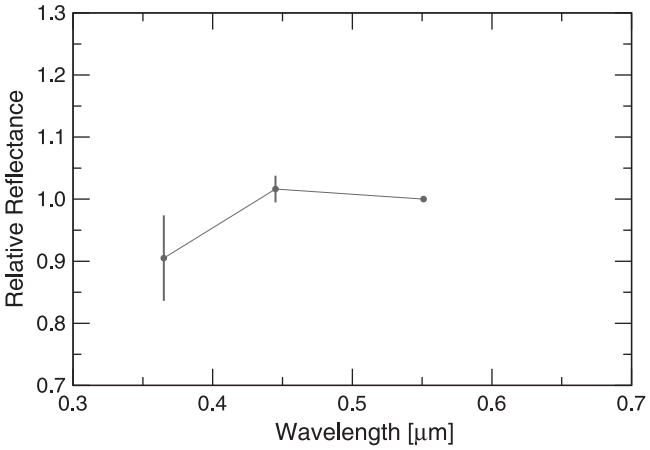

Figure A2. *UBV* colors for (701) Oriola from Bowell et al. (1979), normalized at 0.55 μm. The taxonomy is classified as C type (Tholen 1984, 1989).

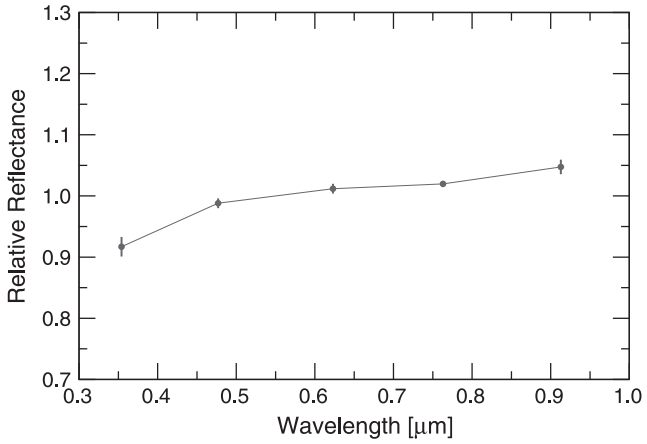

Figure A3. Visual colors of asteroid (2542) Calpurnia taken by SDSS (Hasselmann et al. 2012). The relative colors scaled to 1.0 at 0.55 μm are compatible with C type.

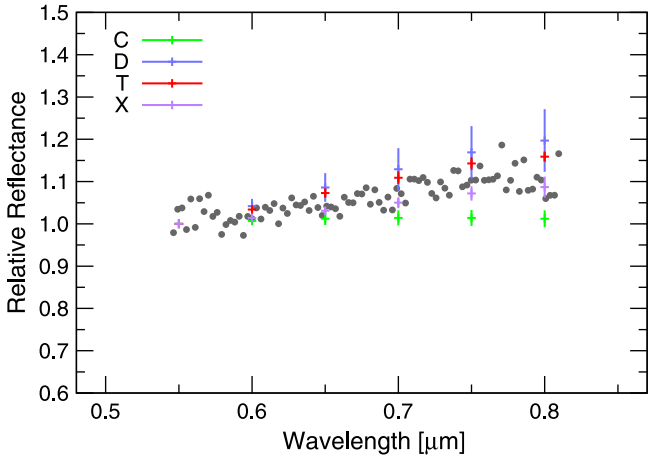

Figure A4. Comparison between the optical spectra of asteroid (2670) Chuvashia and those of C, D, T, and X(M) types taken from the Bus–DeMeo taxonomy database (DeMeo et al. 2009). All data are normalized at 0.55 μm. The asteroid is conceivably related in appearance to either D/T- or M-type asteroids.

28. We used the 1.88 m telescope located in Okayama, Japan (133° 33′38 24″ W, 34° 34′ 37″47 N). The Kyoto Okayama Optical Low-dispersion Spectrograph (KOOLS) in long-slit spectroscopy mode was operated (Ohtani et al. 1998; Ishigaki et al. 2004). An A SITe ST-002 A 2048 × 4096 was employed at the Cassegrain focus. We used a 2 × 2 binned spatial scale of 0″668 pixel^{-1} in the spectroscopic mode. A slit width of 6” (grism No.2) was used for the spectroscopy, of which coverage was from 0.55 to 0.80 μm with a spectral resolving power of 180–240. We obtained spectra at heliocentric and geocentric distances of 3.053 AU and 2.253 AU, respectively, and with a phase angle = 12.6°. Exposure times are 1200 s, and we took three images of the asteroid and combined them to improve the signal-to-noise ratio. The data were spectrally calibrated using the solar analog SA102-1081(G type). We took an eight binned wavelength scale for the spectrum.

We show in figure A4 the spectrum of asteroid (2670) Chuvashia and compare it with that of C, D, T, and X types in the Bus–DeMeo taxonomy system (DeMeo et al. 2009). Since the T type is included within the uncertainties of the D type, we use the expression D/T type. For the asteroids herein, X type is

considered to be M type based on the definition in visual albedos (0.1–0.3) by Tholen (1984). The spectrum of (2670) falls between D/T- and M-type asteroids.

REFERENCES

A'Hearn, M. F., & Feldman, P. D. 1992, Icar, 98, 54
Bell, J. F., Davis, D. R., Hartmann, W. K., & Gaffey, M. J. 1989, in Asteroids II, ed. R. P. Binzel, T. Gehrels, & M. S. Matthews (Tucson: Univ. Arizona Press), 921
Bendjoya, P., Cellino, A., di Martino, M., & Saba, L. 2004, Icar, 168, 374
Berger, E. L., Zega, T. J., Keller, L. P., & Lauretta, D. S. 2011, GeCoA, 75, 3501
Bishop, J. L., & Pieters, C. M. 1995, JGR, 100, 5369
Bodewits, D., Vincent, J.-B., & Kelley, M. S. P. 2014, Icar, 229, 190
Bodewits, D., Kelley, M. S., Li, J.-Y., et al. 2011, ApJL, 733, L3
Bowell, E., Gehrels, T., & Zellner, B. 1979, in Asteroids, ed. T. Gehrels (Tucson: Univ. Arizona Press), 1108
Brearley, A. J. 2006, in Meteorites and the Early Solar System II, Vol. 943, ed. D. S. Lauretta, & H. Y. McSween, Jr. (Tucson: Univ. Arizona Press), 584
Brownlee, D., Tsou, P., Aléon, J., et al. 2006, Sci, 314, 1711
Bus, S. J. 1999, PhD thesis, Massachusetts Institute of Technology
Bus, S. J., & Binzel, R. P. 2002a, Icar, 158, 106
Bus, S. J., & Binzel, R. P. 2002b, Icar, 158, 146
Campins, H., Hargrove, K., Pinilla-Alonso, N., et al. 2010, Natur, 464, 1320
Carruba, V. 2013, MNRAS, 431, 3557
Clark, R. N., & Lucey, P. G. 1984, JGR, 89, 6341
Cruikshank, D. P., Dalle Ore, C. M., Roush, T. L., et al. 2001, Icar, 153, 348
de León, J., Pinilla-Alonso, N., Campins, H., Licandro, J., & Marzo, G. A. 2012, Icar, 218, 196
DeMeo, F., & Binzel, R. P. 2008, Icar, 194, 436
DeMeo, F. E., Binzel, R. P., Slivan, S. M., & Bus, S. J. 2009, Icar, 202, 160
DeMeo, F. E., & Carry, B. 2013, Icar, 226, 723
Dorschner, J., Begemann, B., Henning, T., Jaeger, C., & Mutschke, H. 1995, A&A, 300, 503
Dotto, E., Fornasier, S., Barucci, M. A., et al. 2006, Icar, 183, 420
Emery, J. P., & Brown, R. H. 2003, Icar, 164, 104
Emery, J. P., & Brown, R. H. 2004, Icar, 170, 131
Fernández, Y. R., Jewitt, D. C., & Sheppard, S. S. 2005, AJ, 130, 308
Fornasier, S., Clark, B. E., Dotto, E., et al. 2010, Icar, 210, 655
Gaffey, M. J., & McCord, T. B. 1978, SSRv, 21, 555
Gaffey, M. J., Burbine, T. H., & Binzel, R. P. 1993, Metic, 28, 161
Gradie, J., & Tedesco, E. 1982, Sci, 216, 1405
Hanner, M. S. 1999, SSRv, 90, 99
Hapke, B. 1981, JGR, 86, 3039
Hapke, B. 1993, in Theory of Reflectance and Emittance Spectroscopy (Cambridge: Cambridge Univ. Press)
Hapke, B. 2012, in Theory of Reflectance and Emittance Spectroscopy (2nd ed.; Cambridge: Cambridge Univ. Press)
Hasegawa, S., Murakawa, K., Ishiguro, M., et al. 2003, GeoRL, 30, 2
Hasselmann, P. H., Carvano, J. M., & Lazzaro, D. 2012, SDSS-based Asteroid Taxonomy V1.1. EAR-A-I0035–5-SDSSTAX-V1.1. NASA Planetary Data System, http://sbn.psi.edu/pds/resource/sdsstax.html
Hayano, Y., Takami, H., Oya, S., et al. 2010, Proc. SPIE, 7736, 21
Hiroi, T., Pieters, C. M., Zolensky, M. E., & Lipschutz, M. E. 1993, Sci, 261, 1016
Hiroi, T., Zolensky, M. E., Pieters, C. M., & Lipschutz, M. E. 1996, M&PS, 31, 321
Hsieh, H. H., & Jewitt, D. 2006, Sci, 312, 561
Ishigaki, T., Hayashi, T., Ohtani, H., et al. 2004, PASJ, 56, 723
Ishiguro, M., Hanayama, H., Hasegawa, S., et al. 2011, ApJL, 740, L11
Jessberger, E. K. 1999, SSRv, 90, 91
Jewitt, D. C. 2002, AJ, 123, 1039
Jewitt, D. C. 2004, in Comets II, Vol. 745, ed. M. C. Festou, H. U. Keller, & H. A. Weaver (Tucson: Univ. Arizona Press), 659
Jewitt, D. 2012, AJ, 143, 66
Jewitt, D., Chizmadia, L., Grimm, R., & Prialnik, D. 2007, in Protostars and Planets V, ed. B. Reipurth, et al. (Tucson, AZ: Univ. Arizona Press), 863
Jewitt, D., Weaver, H., Mutchler, M., Larson, S., & Agarwal, J. 2011, ApJL, 733, L4
Jones, T. D., Lebofsky, L. A., Lewis, J. S., & Marley, M. S. 1990, Icar, 88, 172
Kamei, A., & Nakamura, A. M. 2002, Icar, 156, 551
Kasuga, T., Watanabe, J., & Ebizuka, N. 2005a, A&A, 438, L17
Kasuga, T., Yamamoto, T., Watanabe, J., et al. 2005b, A&A, 435, 341
Kasuga, T., Balam, D. D., & Wiegert, P. A. 2010, AJ, 140, 1806
Kasuga, T., Usui, F., Ootsubo, T., Hasegawa, S., & Kuroda, D. 2013, AJ, 146, 1
Kelley, M. S., & Wooden, D. H. 2009, P&SS, 57, 1133
Kobayashi, N., Tokunaga, A. T., Terada, H., et al. 2000, Proc. SPIE, 4008, 1056
Küppers, M., et al. 2014, Natur, 505, 525
Lamy, P., & Toth, I. 2009, Icar, 201, 674
Lamy, P. L., Toth, I., Fernandez, Y. R., & Weaver, H. A. 2004, in Comets II, Vol. 745, ed. M. C. Festou, H. U. Keller, & H. A. Weaver (Tucson, AZ: Univ. Arizona Press), 223
Lazzaro, D., Angeli, C. A., Carvano, J. M., et al. 2004, Icar, 172, 179
Licandro, J., Campins, H., Kelley, M., et al. 2011, A&A, 525, A34
Lisse, C. M., VanCleve, J., Adams, A. C., et al. 2006, Sci, 313, 635
Lucey, P. G., & Noble, S. K. 2008, Icar, 197, 348
Masiero, J. R., Mainzer, A. K., Grav, T., et al. 2011, ApJ, 741, 68
Masiero, J. R., Mainzer, A. K., Grav, T., et al. 2012, ApJL, 759, L8
Masiero, J. R., Grav, T., Mainzer, A. K., et al. 2014, ApJ, 791, 121
McCord, T. B., Li, J.-Y., Combe, J.-P., et al. 2012, Natur, 490, 83
McKinnon, W. B., Prialnik, D., Stern, S. A., & Coradini, A. 2008, in The Solar System Beyond Neptune, ed. M. A. Barucci, H Boehnhardt, D. P. Cruikshank, & A Morbidelli (Tucson, AZ: Univ. Arizona Press), 213
McSween, H. Y., Jr., Ghosh, A., Grimm, R. E., Wilson, L., & Young, E. D. 2002, in Asteroids III, ed. W. F. Bottke, A. Cellino, Jr., P. Paolicchi, & R. P. Binzel (Tucson, AZ: Univ. Arizona Press), 559
Merk, P., & Prialnik, D. 2006, Icar, 183, 283
Miles, R., & Faillace, G. A. 2012, Icar, 219, 567
Minowa, Y., Hayano, Y., Oya, S., et al. 2010, Proc. SPIE, 7736, 122
Mothe-Diniz, T., Roig, F., & Carvano, J. M. 2012, Mothe-Diniz Asteroid Dynamical Families V1.1. EAR-A-VARGBDET-5-MOTHEFAM-V1.1. NASA Planetary Data System, http://sbn.psi.edu/pds/resource/mothefam.html
Nakamura-Messenger, K., Clemett, S. J., Messenger, S., & Keller, L. P. 2011, M&PS, 46, 843
Nakamura, T., Noguchi, T., Tsuchiyama, A., et al. 2008, Sci, 321, 1664
Nesvorny, D. 2012, Nesvorny HCM Asteroid Families V2.0, EAR-A-VARGBDET-5-NESVORNYFAM-V2.0, NASA Planetary Data System, 189
Novakovic, B. 2011, PhD thesis Univ. of Belgrade
Ohtani, H., Ishigaki, T., Maemura, H., et al. 1998, Proc. SPIE, 3355, 750
Ootsubo, T., Kawakita, H., Hamada, S., et al. 2012, ApJ, 752, 15
Prialnik, D., & Podolak, M. 1999, SSRv, 90, 169
Prialnik, D., Sarid, G., Rosenberg, E. D., & Merk, R. 2008, SSRv, 138, 147
Pollack, J. B., Hollenbach, D., Beckwith, S., et al. 1994, ApJ, 421, 615
Rietmeijer, F. J. M. 1985, Natur, 313, 293
Rivkin, A. S., & Emery, J. P. 2010, Natur, 464, 1322
Rivkin, A. S., Howell, E. S., Vilas, F., & Lebofsky, L. A. 2002, in Asteroids III, ed. W. F. Bottke, Jr., A. Cellino, P. Paolicchi, & R. P. Binzel (Tucson, AZ: Univ. Arizona Press), 235
Rivkin, A. S., Howell, E. S., Emery, J. P., Volquardsen, E. L., & DeMeo, F. E. 2012, AGU abstract, #P31A-1878
Rivkin, A. S., Howell, E. S., Emery, J. P., Volquardsen, E. L., & DeMeo, F. E. 2012, EPSC id. EPSC2012–359
Rouleau, F., & Martin, P. G. 1991, ApJ, 377, 526
Roush, T. L. 1994, Icar, 108, 243
Ryan, E. L., & Woodward, C. E. 2010, AJ, 140, 933
Szabó, G. M., Ivezić, Ž., Jurić, M., & Lupton, R. 2007, MNRAS, 377, 1393
Takir, D., & Emery, J. P. 2012, Icar, 219, 641
Tedesco, E. F., Noah, P. V., Noah, M., & Price, S. D. 2002, AJ, 123, 1056
Terada, H., Kobayashi, N., Tokunaga, A. T., et al. 2004, Proc. SPIE, 5492, 1542
Tholen, D. J. 1984, PhD thesis, Arizona Univ., Tucson
Tholen, D. J. 1989, in Asteroids II, ed. P. B. Richard, G. Tom, & S. M. Mildred (Tucson, AZ: Univ. Arizona Press), 1139
Tokunaga, A. T., Kobayashi, N., Bell, J., et al. 1998, Proc. SPIE, 3354, 512
Usui, F., Kuroda, D., Müller, T. G., et al. 2011, PASJ, 63, 1117
Usui, F., Kasuga, T., Hasegawa, S., et al. 2013, ApJ, 762, 56
Vernazza, P., Mothé-Diniz, T., Barucci, M. A., et al. 2005, A&A, 436, 1113
Vilas, F., & Gaffey, M. J. 1989, Sci, 246, 790
Weisberg, M. K., McCoy, T. J., & Krot, A. N. 2006, in Meteorites and The Early Solar System II, Vol. 943, ed. D. S. Lauretta, & H. Y. McSween, Jr. (Tucson: Univ. Arizona Press), 19
Wooden, D. H. 2008, SSRv, 138, 75
Yamamoto, T. 1985, A&A, 142, 31
Yang, B., & Jewitt, D. 2007, AJ, 134, 223
Yang, B., & Jewitt, D. 2010, AJ, 140, 692
Yang, B., & Jewitt, D. 2011, AJ, 141, 95
Yang, B., Lucey, P., & Glotch, T. 2013, Icar, 223, 359
Zolensky, M. E., Zega, T. J., Yano, H., et al. 2006, Sci, 314, 1735
Zolensky, M. E., Nakamura-Messenger, K., Rietmeijer, F., et al. 2008, M&PS, 43, 261